

Coupled quantum electrodynamics in photonic crystal nanocavities

Y.-F. Xiao^{1,2,*}, J. Gao¹, X.-B. Zou², J. F. McMillan¹, X. Yang¹,

Y.-L. Chen², Z.-F. Han², G.-C. Guo², and C. W. Wong^{1†}

¹*Optical Nanostructures Laboratory, Columbia University, New York, NY 10027 and*

²*Key Laboratory of Quantum Information, University of Science and Technology of China, P. R. China*

We show that a scalable photonic crystal nanocavity array, in which single embedded quantum dots are coherently interacting, can perform as a universal single-operation quantum gate. In a passive system, the optical analogue of electromagnetically-induced-transparency is observed. The presence of a single two-level system in the array dramatically controls the spectral lineshapes. When each cavity couples with a two-level system, our scheme achieves two-qubit gate operations with high fidelity and low photon loss, even in the bad cavity limit and with non-ideal detunings.

PACS numbers: 03. 67.-a, 42.50. Pq, 85.35.Be, 42.70.Qs

Introduction.—Cavity quantum electrodynamics (QED) describes a small number of atoms strongly coupling to quantized electromagnetic fields through dipolar interactions inside an optical cavity. Up to now, it is one of few experimentally realizable systems in which the intrinsic quantum mechanical coupling dominates losses due to dissipation, providing an almost ideal system which allows quantitative studying of a dynamical open quantum system under continuous observation. In the strongly coupled regime, quantum state mapping between atomic and optical states becomes possible, which has promising implications towards realization of chip-scale quantum information processing [1]. Over the past few years, theoretical and experimental interests are mainly focused on a single cavity interacting with atoms, and important successes have been made ranging from trapping of strongly coupled single atoms inside an optical microcavity [2] and deterministic generation of single-photon states [3], to observation of atom-photon quantum entanglement [4] and implementation of quantum communication protocols [5].

For more applications in cavity QED, current interest lies in the coherent interaction among several distant cavities. The coherent interaction of cavity arrays has been studied as a classical analogy to electromagnetically induced transparency (EIT) in both theory [6, 7] and experiment [8, 9]. Coupled cavities can be utilized for coherent optical information storage because they provide almost lossless guiding and coupling of light pulses at ultrasmall group velocities. When dopants such as atoms or quantum dots (QDs) interacts with these cavities, the spatially separated cavities have been proposed for implementing quantum logic and constructing quantum networks [10]. Recent studies also show a photon-blockade regime and Mott insulator state [11], where the two-dimensional hybrid system undergoes a characteristic Mott insulator (excitations localized on each site) to superfluid (excitations delocalized across the lattice) quantum phase transition at zero temperature [12]. The character of a coupled cavity configuration has also been

studied using the photon Green function [13, 14].

Theoretical model.—In this paper, using transmission theory we study coherent interactions in a cavity array which includes N nanocavity-QD subsystems, with indirect coupling between adjacent cavities through a waveguide (Fig. 1), and examine its implementation as a two-qubit single-operation quantum gate. Recent experimental efforts have reported remarkable progress in solid-state nanocavities, such as an ultrahigh quality factor [15, 16], observation of strong coupling and vacuum Rabi splitting [17, 18], transfer of single photons between two cavities [19], and deterministic positioning of a cavity mode with respect to a QD [20].

First, we investigate a subsystem in which a single nanocavity interacts with an isolated QD. Here for simplicity we suppose that only a single optical resonance mode (h -polarized) is present in the nanocavity, although two-mode cavity-QD interactions have been considered earlier [21]. The nanocavity-QD-waveguide subsystem

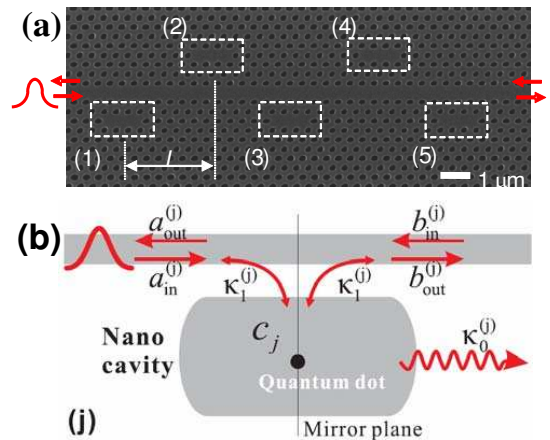


FIG. 1: (color) (a) Example scanning electronic micrograph of periodic waveguide-resonator structure containing N side-coupled nanocavities (h -polarized) at a distance L . The nanocavities are side coupled through the integrated waveguide, with no direct coupling between any two nanocavities. (b) The j -th QD-cavity subsystem.

has mirror-plane symmetry, so that the mode is even with respect to the mirror plane. Omitting the terms which concern the Langevin noises, we can easily obtain Heisenberg equations of motion [22]

$$\frac{dc_j}{dt} = -i[c_j, H_j] - \Gamma_j c_j + i\sqrt{\kappa_{1,j}}(a_{\text{in}}^{(j)} + b_{\text{in}}^{(j)}), \quad (1)$$

$$\frac{d\sigma_{-,j}}{dt} = -i[\sigma_{-,j}, H_j] - \gamma_j \sigma_{-,j}, \quad (2)$$

where c_j is bosonic annihilation operator of the j -th cavity mode with resonant frequency $\omega_{c,j}$. $a_{\text{in}}^{(j)}(b_{\text{in}}^{(j)})$ and $a_{\text{out}}^{(j)}(b_{\text{out}}^{(j)})$ describe the input and output fields in the left (right) port respectively. $2\Gamma_j$ represents total cavity decay with $\Gamma_j = (\kappa_{0,j} + 2\kappa_{1,j})/2$, where $\kappa_{0,j}$ is the intrinsic cavity decay rate and $\kappa_{1,j}$ the external cavity decay rate. $\sigma_{-(+),j}$ is the descending (ascending) operator of the interacting two-level QD with transition frequency $\omega_{r,j}$. γ_j is the total decay rate of the QD, including the spontaneous decay (at rate γ_s) and dephasing (at rate γ_p) in the excited state $|e\rangle$; H_j is the subsystem Hamiltonian $H_j = \omega_{c,j}c_j^\dagger c_j + \omega_{r,j}\sigma_{+,j}c_j + [g_j(\vec{r})\sigma_{+,j}c_j + h.c.]$, where $g_j(\vec{r})$ is the coupling strength between the cavity mode and the dipolar transition $|g\rangle \leftrightarrow |e\rangle$.

Our scheme operates in the weak excitation limit (excited by a weak monochromatic field or a single photon pulse with frequency ω), so that the motion equations can be solved, with the transport relation

$$\begin{pmatrix} b_{\text{in}}^{(j)}(\omega) \\ b_{\text{out}}^{(j)}(\omega) \end{pmatrix} = T_j \begin{pmatrix} a_{\text{in}}^{(j)}(\omega) \\ a_{\text{out}}^{(j)}(\omega) \end{pmatrix}. \quad (3)$$

Here the transport matrix is

$$T_j = \frac{1}{\alpha_j + \kappa_{1,j} - \Gamma_j} \begin{pmatrix} -\kappa_{1,j} & \alpha_j - \Gamma_j \\ \alpha_j - \Gamma_j + 2\kappa_{1,j} & \kappa_{1,j} \end{pmatrix}, \quad (4)$$

where $\alpha_j = i\Delta_{c,j} + |g_j(\vec{r})|/(i\Delta_{r,j} - \gamma_j)$, and $\Delta_{c,j} = \omega - \omega_{c,j}$ ($\Delta_{r,j} = \omega - \omega_{r,j}$) represents the detuning between the input field and the cavity mode (QD transition). The transport matrix can be regarded as a basic cell in cascading the subsystems and obtaining the whole transportation for the N -coupled cavity-QD system. The transport properties can thus be expressed as

$$\begin{pmatrix} b_{\text{in}}^{(N)}(\omega) \\ b_{\text{out}}^{(N)}(\omega) \end{pmatrix} = T_N T_0 \cdots T_0 T_2 T_0 T_1 \begin{pmatrix} a_{\text{in}}^{(1)}(\omega) \\ a_{\text{out}}^{(1)}(\omega) \end{pmatrix}, \quad (5)$$

where T_0 is the transport matrix via the waveguide with a propagation phase θ . Eq. (5) is an important result in this paper, and in the following we will show that it can be used in various interesting physical processes.

Spectral character of coupled QD-cavity arrays.—To examine the physical essence, we first examine the spectral character of the coupled QD-cavity system. The reflection and transmission coefficients are defined as $r_{N1} \equiv a_{\text{out}}^{(1)}/a_{\text{in}}^{(1)}$ and $t_{N1} \equiv b_{\text{out}}^{(N)}/a_{\text{in}}^{(1)}$. We also assume

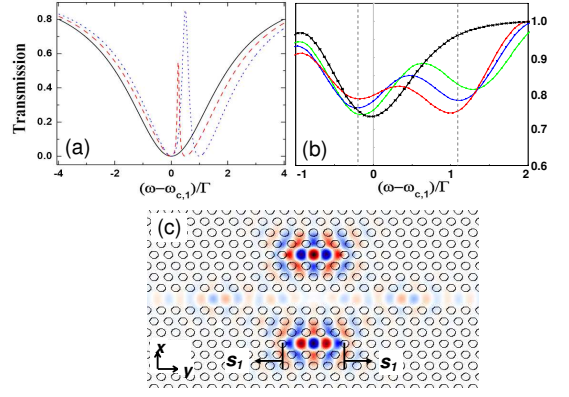


FIG. 2: (color) (a) and (b): Transmission spectra of two coupled empty nanocavities. Solid, dashed, and dotted lines describe the cases of $\delta_{21} = 0, \Gamma/2, \Gamma$, respectively. The used parameters: $\gamma = \kappa_0, \theta = 20\pi$. (b) Numerical 3D FDTD simulations of optical analogue of EIT in two coherently coupled cavity ($\theta = 0$) for detunings 1.14Γ (red; $\Delta\epsilon_{\text{cavities}} = 0.135$), 1.26Γ (blue; $\Delta\epsilon_{\text{cavities}} = 0.160$), and 1.49Γ (green; $\Delta\epsilon_{\text{cavities}} = 0.185$). The arrows denote the EIT peak transmissions. The dashed grey lines denote the two detuned individual resonances for the case of $s_1 = 0.05a$. The black curve is for a single cavity transmission for reference. (c) Example E_x -field distribution of coupled empty photonic crystal nanocavities.

that these cavities possess the same dissipation characteristic, i.e., $\kappa_{0,j} = \kappa_0, \kappa_{1,j} = \kappa_1, \kappa_1 = 50\kappa_0$, and $\Gamma_j = \Gamma$.

Fig. 2a describes the transmission spectra of two coupled empty cavities with different detuning ($\delta_{21} \equiv \omega_{c,2} - \omega_{c,1}$). When the two cavities are exactly resonant, a transmission dip is observed; with increasing δ_{21} , a sharp peak exists at the center position between the two cavity modes. This is directly analogous to the phenomenon of EIT in atomic vapors, and examined exactly through ab initio 3D finite-difference time-domain (FDTD) numerical simulations. Specifically, Fig. 2b shows an example of the field distributions through the coherent interaction with two coupled empty (without QD) cavities, where the resonance of one cavity is detuned by three cases: $\delta_{21} = 1.14\Gamma, 1.26\Gamma$, and 1.49Γ . The optical EIT-like resonance is observed on top of a background Fabry-Perot oscillation (due to finite reflections at the waveguide facets). The analogy and difference between optical and atomic EIT are recently discussed in Ref. [7].

In the presence of QDs, Fig. 3a (top) shows the spectral characteristics in which a single QD resonantly interacts with the first cavity. When both cavities are resonant, there exist two obvious sharp peaks located symmetrically around $\omega = 0$ (For convenience, we define $\omega_{c,1} = 0$). This fact can be explained by the dressed mode theory. Resonant QD-cavity interaction results in two dressed cavity modes, which are significantly detuned from the second cavity mode with the detuning $\pm |g_1(\vec{r})| = \pm \Gamma/2$. Both dressed modes non-resonantly couple with the second cavity mode, resulting in two

EIT-like peaks located at frequencies $\omega \approx \pm\Gamma/4$. When $\delta_{21} = \Gamma/2$, one dressed cavity mode non-resonantly couples with the second cavity mode with a detuning Γ , which leads to an EIT-like peak located near $\omega \simeq 0$; while the other dressed mode resonantly couples with the second cavity mode, which does not result in an EIT-like spectrum. When δ_{21} continually increases, e.g., $\delta_{21} = \Gamma$, the vanished peak reappears since the two dressed modes are always non-resonant with the second cavity mode. Fig. 3a (bottom) illustrates the case where both cavities resonantly interact with a single QD each. Similar to the above analysis, we can explain the number and locations of sharp peaks with respect to different δ_{21} by comparing the two pairs of dressed cavity modes. For example, when $\delta_{21} = \Gamma$, the dressed modes in the first cavity is located at $\pm\Gamma/2$ while the second pair is at $\Gamma/2$ and $3\Gamma/2$, so that the EIT-like peaks must locate $[-\Gamma/2, \Gamma/2]$ and $[\Gamma/2, 3\Gamma/2]$, i.e., two peaks are near 0 and Γ . Fig. 3b shows the spectral character of three coupled QD-cavity subsystems, under various cavity-cavity and QD-cavity detunings that might be observed experimentally, involving Autler-Townes splittings and Fano interferences.

To further examine this coupled QD-cavity system, Fig. 3c shows the transmission phase shift for various qubit detunings, where the cavity and QD transition are resonant for both subsystems. We find that the phase shift has a steep change, which corresponds to a strong suppression of the flying-qubit group velocity. As shown in Fig. 3d, the delay time (τ_{sto}) in this coupled system is almost hundreds of the cavity lifetime ($\tau_{\text{life}} = 1/2\Gamma$). This proposed coupled QD-cavity system can essentially be applied in storing quantum information of light. Although having shorter coherence times than atomic ion qubit memory [24], our solid-state implementation has an achievable bandwidth of ~ 50 MHz in contrast to less than 100 kHz in atomic systems, with a comparable delay-bandwidth product. One can also consider dynamical tuning [25] to tune the cavity resonances with respect to the QD transitions to break the delay-bandwidth product in our solid-state cavity array system.

Quantum phase gate operation.—Now we show the possibility of quantum gate operation based on the dynamical evolution. In constructing quantum logic system, we have stationary qubits represented by two ground states $|g\rangle$ and $|r\rangle$ of QDs. The two ground states can be obtained via QD spin-states such as shown remarkably in Ref. [26] with near-unity fidelity. To facilitate the discussion but without loss of generality, we consider an all resonance case (i.e., $\omega = \omega_{c(r),j}$) to describe idea of the phase gate operation, and in the subsequently numerical calculation, we will demonstrate the gate feasibility under non-ideal detunings.

As an example, we focus on how to unconditionally realize a stationary two-qubit (two QDs) phase gate. The input weak photon pulse is assumed h -polarized and we should discuss the following cases with different initial

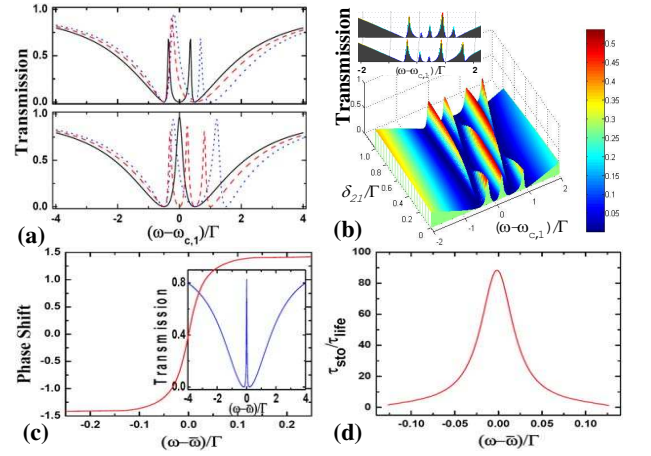


FIG. 3: (color) (a) Transmission spectra of two coupled subsystems with one QD (top) and two QDs (bottom) where $g = \Gamma/2$. Other conditions are same as Fig. 2a. (b) Spectral character of three coupled subsystems with $\delta_{31} = \Gamma/2$. Inset: $\delta_{31} = \Gamma/2$, $\delta_{21} = 0$, $\delta_1 = \delta_3 = 0$, with $\delta_2 = \Gamma/2$ (top) and Γ (bottom), where $\delta_j \equiv \omega_{c,j} - \omega_{r,j}$. (c) and (d): Photon phase shift and delay (τ_{sto}) through two QD-nanocavity subsystems, where $\omega_{c(r),j} = \omega$, $g = 0.2\Gamma$. Inset: transmission spectrum.

QD states. Case I: The two QDs are initially prepared in $|u\rangle_1 |v\rangle_2$ ($u, v = g, r$) and at least one QD occupies the ground state $|r\rangle$. It is not difficult to find $r_{21} \simeq -1$ and $t_{21} \simeq 0$ under the over-coupling regime ($\kappa_0 \ll \kappa_1$) and with large Purcell factor ($g^2/\Gamma\gamma \gg 1$). This fact can be understood by regarding the resonant condition ($\omega_{c,j} = \omega$). The input photon will be almost reflected by one *empty* cavity, in which the QD is in $|r\rangle$, resulting in a final state $-|u\rangle_1 |v\rangle_2 |R\rangle$, where $|R\rangle$ denotes the reflected photon. Case II: The QDs is initially prepared in $|g\rangle_1 |g\rangle_2$. With the over-coupling lifetime and the large Purcell factor, we have $r_{21} \simeq 0$ and $t_{21} \simeq 1$, so that the photon pulse passes through the two cavities in turn via the waveguide, and the resulting state is $|g\rangle_1 |g\rangle_2 |T\rangle$, where $|T\rangle$ describes the transmitted photon. Here note that the spatial mode of the output photon is actually entangled with the QD states. To construct the final gate operation, it is necessary to remove the distinguishability of the two photon spatial modes (transmitted and reflected). Here we introduce a reflecting element in the end of waveguide (such as a heterostructure interface [15], shown in the inset in Fig. 4a), which makes the photon reflected and interacts with the coupled QD-cavity system again. With precisely adjusting the position of the element, the final state can be obtained as $|g\rangle_1 |g\rangle_2 |R\rangle$. Therefore, the QD-QD gate described by $U = e^{i\pi|g\rangle_1 \langle g|_2 |g\rangle_1 \langle g|_2}$, can be manipulated. Most importantly, this idea can also be easily extended to realize an N -qubit gate with also only one step. Note that only N coupled two-level QD-cavities are required to realize arbitrary unitary operation on a 2^N -dimensional state space of N -qubits, compared to $(2^N - 3)$ two-qubit controlled gates without aux-

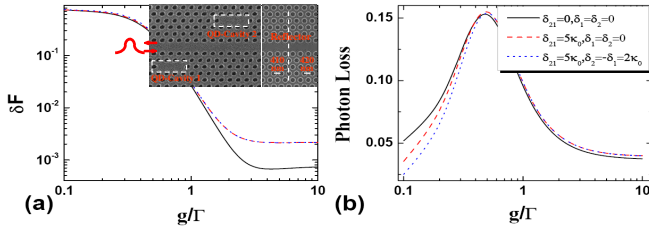


FIG. 4: (color) Gate fidelity change ($\delta F \equiv 1 - F$) (a) and photon loss P (b) of the two-qubit gate versus g/Γ . Inset in (a): a configuration of two-qubit gate operation in which a reflecting element (with 95% reflectivity) is introduced at the end of the QD-cavity subsystem. Here the carrier frequency is assumed as $\omega - 2.5\kappa_0$ to avoid the EIT-like peaks of two coupled empty cavities, and a scattering loss of 1% is used in the short propagation lengths at the slow group velocities. Other parameters are same as Fig. 2a.

iliary qubits [27], which is of importance for reducing the complexity of the physical realization of practical quantum computation and quantum algorithms.

Gate Fidelity and Photon Loss.—To exemplify a two-qubit coupled cavity system, isolated single semiconductor QDs in high- Q small-modal-volume (V) photonic crystal nanocavities are potential candidates, such as self-assembled InAs QDs in GaAs cavities [17, 18, 19, 20], or PbS nanocrystals in silicon cavities at near 1550 nm wavelengths [28]. For PbS nanocrystal and silicon nanocavity material system, we use the following relevant parameters in our calculations: $\gamma_s \sim 2$ MHz, $\gamma_p \sim 1$ GHz at cooled temperatures, $Q \sim 10^6$ as reported experimentally [15], $V \sim 0.1 \mu\text{m}^3$ at 1550 nm, with resulting single-photon coherent coupling rate $g \sim 30$ GHz. To characterize the present gate operation, Figs. 4a and 4b demonstrate a high two-qubit phase gate fidelity F and a small photon losses P for different single-photon coupling rates g , even under a non-ideal detuning condition and bad cavity limit. Based on the above parameters, F can be as high as 0.999, and P can be as low as 0.04. Under various cavity-cavity detunings, both F and P have no significant degradation. Furthermore, even in the presence of the QD-cavity detuning that is comparable with the bare cavity linewidth, both F and P keep almost unchanged. It is remarkable that the on-resonance P is even larger than the non-resonance case when g is small. This can be explained by considering the decay of QDs. When the QDs resonantly interact with cavity modes, the decay of QDs becomes distinct, which results in an increasing of photon loss. On the other hand, P exhibits an increase before a decrease with increasing g , which can be understood by studying the photon loss when the QDs are in the state of $|g\rangle_1 |g\rangle_2$. When $g \simeq \Gamma/2$, the absorption strength (resulted κ_0 from γ) of the input photon by the coupled cavities reaches the maximum.

Conclusion.—We have introduced and examined the coherent interaction of a two-qubit quantum phase gate

in a realizable solid-state nanocavity QED system. The coupling of a nanoscale emitter to the quantized cavity mode in a coherent array results in unique lineshapes and can give an important indication of the interactions. Significantly, the fidelity and photon loss of the gate are kept within tolerable bounds even in a realistic semiconductor material system. This provides an approach towards a chip-scale quantum network for large-scale quantum information storage and computation.

The authors acknowledge funding support from DARPA, and the New York State Office of Science, Technology and Academic Research.

* Electronic address: yfxiao@ustc.edu.cn

† Electronic address: cww2104@columbia.edu

- [1] For a review, see H. Mabuchi and A. C. Doherty, *Science* **298**, 1372 (2002), and references therein.
- [2] J. McKeever *et al.*, *Phys. Rev. Lett.* **90**, 133602 (2003).
- [3] M. Keller *et al.*, *Nature (London)* **431**, 1075 (2004); J. McKeever *et al.*, *ibid.* **303**, 1992 (2004); A. Kuhn, M. Hennrich, and G. Rempe, *Phys. Rev. Lett.* **89**, 067901 (2002).
- [4] J. Volz *et al.*, *Phys. Rev. Lett.* **96**, 030404 (2006).
- [5] W. Rosenfeld, S. Berner, J. Volz, M. Weber, and H. Weinfurter, *Phys. Rev. Lett.* **98**, 050504 (2007).
- [6] D. D. Smith, H. Chang, K. A. Fuller, A. T. Rosenberger, and R. W. Boyd, *Phys. Rev. A* **69**, 063804 (2004).
- [7] Y.-F. Xiao *et al.*, *Phys. Rev. A* **75**, 063833 (2007).
- [8] Q. Xu *et al.*, *Phys. Rev. Lett.* **96**, 123901 (2006).
- [9] K. Totska, N. Kobayashi, and M. Tomita, *Phys. Rev. Lett.* **98**, 213904 (2007).
- [10] J. I. Cirac, P. Zoller, H. J. Kimble, and H. Mabuchi, *Phys. Rev. Lett.* **78**, 3221 (1997); W. Yao, R. Liu, and L. J. Sham, *ibid.* **95**, 030504 (2005); A. Serafini, S. Mancini, and S. Bose, *ibid.* **96**, 010503 (2006).
- [11] M. J. Hartmann, F. G. S. L. Brandao and M. B. Plenio, *Nature Physics* **2**, 849 (2006).
- [12] D. Greentree, C. Tahan, J. H. Cole, L. C. L. Hollenberg, *Nature Physics* **2**, 856 (2006).
- [13] S. Hughes, *Phys. Rev. Lett.* **98**, 083603 (2007).
- [14] F. M. Hu, Lan Zhou, Tao Shi, and C. P. Sun, *Phys. Rev. A* **76**, 013819 (2007).
- [15] S. Noda, M. Fujita, and T. Asano, *Nature Photonics* **1**, 449 (2007).
- [16] T. Tanabe, M. Notomi, E. Kuramochi, A. Shinya, H. Taniyama, *Nature Photonics* **1**, 49 (2007).
- [17] T. Yoshie *et al.*, *Nature* **432**, 200 (2004).
- [18] K. Hennessy *et al.*, *Nature* **445**, 896 (2007).
- [19] D. Englund *et al.*, *Opt. Express* **15**, 5550 (2007).
- [20] A. Badolato *et al.*, *Science* **308**, 1158 (2006).
- [21] Y.-F. Xiao *et al.*, *Appl. Phys. Lett.* **91**, 151105 (2007).
- [22] E. Waks and J. Vuckovic, *Phys. Rev. A* **73**, 041803 (2006).
- [23] H. A. Haus, *Waves and Fields in Optoelectronics*. (Prentice-Hall, Englewood Cliffs, N.J., 1984).
- [24] C. Langer *et al.*, *Phys. Rev. Lett.* **95**, 060502 (2005).
- [25] M. F. Yanik and S. Fan, *Phys. Rev. Lett.* **93**, 233903 (2004); Q. Xu *et al.*, *Nature Physics* **3**, 406 (2007).
- [26] M. Atatuer *et al.*, *Science* **312**, 551 (2006).

- [27] M. L. Nielsen and I. L. Chuang, Quantum Computation and Quantum Information, Cambridge University Press, Cambridge, England, 2000.
- [28] R. Bose *et al.*, Appl. Phys. Lett. **90**, 111117 (2007).